The final 112-frame movie of the 43 GHz SiO masers around the Mira Variable TX Cam

Ioannis Gonidakis[1] Philip J. Diamond[1] and Athol J. Kemball[2]

[1]CSIRO Astronomy and Space Science
Vimiera and Pembroke Roads, Marsfield NSW 2122, Australia
email: `ioannis.gonidakis@csiro.au`

[2]Dept. of Astronomy, University of Illinois at Urbana-Champaign
1002 W. Green Street, Urbana, IL 61801, USA

Abstract. The proximity of the SiO masers to the star, makes them a powerful tool for studying the properties of the extended stellar atmosphere. This project is a long monitoring campaign of the 43 GHz SiO masers (v=1 J=1→0) around the Mira Variable TX Cam. The target source was observed with the Very Long Baseline Array (VLBA) from the 24th of May 1997 to the 25th of January 2002 in bi-weekly or monthly intervals, covering 3.06 stellar cycles. The time-span and frequency of observations helped us examine the long and short-term properties of the emission and study the dynamics of the gas, the existence of shock waves and their contribution to the morphology and kinematics. Maps from each epoch were concatenated into a 112-frame movie showing the evolution of the emission around TX Cam.

Keywords. masers, shock waves, techniques:high angular resolution, techniques:interferometric, stars:AGB and post-AGB, stars:imaging, stars:winds and outflows, stars:circumstellar matter, radio lines:stars

1. Introduction

The first high resolution images of the 43 GHz SiO masers around late-type stars were produced by Diamond *et al.* (1994). Their VLBA observations of the Miras TX Cam and U Her revealed that the masers are confined in well defined rings, overruling the until then prevailing belief that SiO masers form chaotic structures in variable stars. They showed that they form at 2-4 R$_\star$, placing the masers in the extended atmosphere of the stars, within the dust formation zone. The main kinematic behaviour seemed to be that of outflow, with the gas confined in an ellipsoidal region; the maser effect is dominant on the thicker parts of the ellipsoid along our line of side, thus the emission appeared confined in a projected ring.

The first movie of the TX Cam monitoring campaign was published by Diamond & Kemball in 2003. This 44-frame version was covering a complete stellar pulsation cycle at an angular resolution of ∼0.1 mas and revealed the gross kinematic properties of the SiO maser emission. The morphology of the shell appeared to vary with time and some of its properties appeared dependant on the stellar phase. Individual maser features persisted over many epochs and the predominant kinematic behaviour of the ring was that of expansion. Contrary to the models that assume spherical symmetry, the structure and evolution of the ring revealed a high degree of asymmetry. There was also evidence of ballistic deceleration and proper motion analysis revealed motions between ∼5-10%, distributed randomly around the ring.

The 73-frame movie by Gonidakis *et al.* (2010) uncovered more properties of the morphology and the kinematics of the masering shell. Covering two pulsation cycles, the

240

movie revealed another kinematic motion of the ring; contraction was following expansion during the second cycle. The time-span of the movie allowed the study of short- and long-term variability properties, i.e. changes not only within a cycle but also from one cycle to another. The 43 GHz flux variability follows that of the optical with a ∼10% lag but the fluxes are uncorrelated. The width of the ring was also correlated with the stellar pulsation and there was no correlation between the velocities and position angle of the ring. The lifetime of individual components followed a Gaussian distribution with a peak between 150 and 200 days.The spectra were dominated by blue and red-shifted peaks that formed at different times in the stellar cycle and had different lifetimes.

2. Observations and Data Reduction

We observed the *v=1, J=1→0* masers on TX Cam with the VLBA and one antenna from the VLA. Observations started on the 24th of May 1997 and until the 9th of September 1999 were conducted in biweekly intervals; from that date until the end of the project on the 25th of January 2002 observations occurred every month. In total 80 individual data-sets were collected that corresponded to a coverage of 3.06 pulsation periods, given a period of 557 days for TX Cam.

The rest frequency of observations for all epochs was 43.122027 GHz, centred at an LSR velocity of 9.0 km s^{-1}. Within each 6-8 hours scan several sources were observed; 2.5-3.5 hours of each scan were devoted to TX Cam and the rest to calibrators and the other target sources. In order to get all 4 Stokes polarisation data after correlation with the VLBA correlator, we observed in dual polarisation over a 4 MHz bandwidth. The output was 128 spectral channels, thus a spectral resolution of 31.25 kHz corresponding to a velocity resolution of 0.217 km s^{-1}.

There were a number of problems and limitations that made the compilation of the movie a very challenging task. Firstly, we had to ensure that data were recorded and analysed in a consistent and uniform manner. The former was dealt by keeping the same configuration during each experiment as described in the previous paragraph. The latter demanded the creation of an automated procedure, that was developed as a POPS script within the AIPS package and was based on the technique described by Kemball, Diamond and Cotton (1995) and Kemball & Diamond (1997). The pipeline was divided into logical steps and demanded minimum interaction by the user, which was limited to

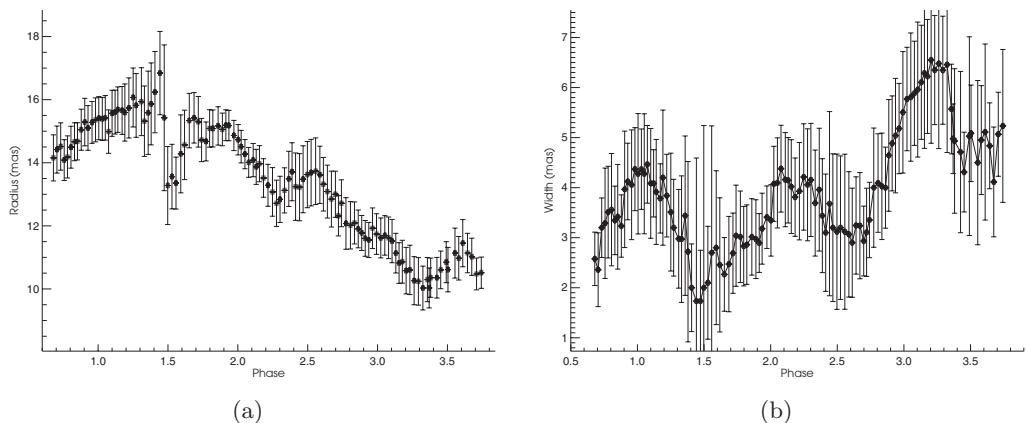(a)   (b)

Figure 1: (a) Plot showing the inner shell radius with the stellar phase. (b) Plot showing the change in the ring's width with the stellar phase.

the examination of the results at the end of each step and the editing. The result was a 128-channel cube of 1024×1024 pixels in R.A and Dec. with a pixel separation of 0.1 mas. However, due to self-calibration any information on the absolute position was lost and the frames were aligned using a two-step approach. During the first step the frames were superimposed and shifted in order to be aligned on a by-eye estimate. Then we used task XYCOR in AIPS that provided a sub-pixel approximation of the needed shift. Once all the images were aligned we had to introduce frames to insure the time-coherence of the movie. For missing epoch or bad data, frames were interpolated with task COMB in AIPS.

3. The Movie

The movie consists of 112 frames and a 10% sample is plotted in Fig. 2. The plots correspond to every tenth frame of the movie that covers three complete stellar cycles spread over four pulsation periods.

3.1. *General Characteristics*

As previously observed, radiation is confined in a ring-like structure around the star that changes in luminosity and shape. The change in luminosity follows the stellar pulsation but the changes in shape are not correlated with the pulsation of the star. The masering zone starts as a ring in the first cycle, resembles an ellipsoid in cycles two and three end ends up as a ring again in cycle four. During the first half of the movie maser emission is mainly located in bright spots, in the second half though bright filaments appear to be the main hosts of emission. Diffuse emission is occasionally apparent, especially during the first cycle and is located at the outer parts of the structure. The flow of the material appears to follow ordered motions, favouring a specific kinematic behaviour along the ring perimeter. Despite this uniform behaviour, there are features that deviate and their effect in the overall appearance of the ring is evident. Characteristic examples are the gash in the eastern part of the ring (ϕ=1.47) and the split in the northeast (ϕ=2.02).

3.2. *Variability*

The characteristics of the masering region appear to change with the stellar phase, some of them in correlation while some randomly. Fig. 1 is a plot of the inner shell radius with respect to the stellar phase. This is a justification of what was visually observed in the movie; the first cycle is dominated by expansion but in the remaining cycles both expansion and contraction are apparent. The radius at which the ring forms is not correlated to the phase so in each cycle the inner boundary can reach significantly different maximum and minimum distances from the center of the star. For example, in the first cycle the ring appears further from the center of the star than in the last. The radius is correlated with the intensity and during more intense cycles the rings form closer to the star.

Fig. 1 shows the change of the ring width with the stellar phase. Despite a lag of ~10%, the width follows the pulsation of the star so, it appears wider at maxima and narrower at minima. The width of the ring is correlated to the intensity of the masers so stronger cycles have wider rings. This explains the much wider ring at the final maximum compared to the others. The width of the ring is also dependant on the radius at which it is formed. Thus, rings closer to the star (which are brighter according to the previous paragraph) are wider too.

It is apparent from the above that the radius of the ring, its width and its intensity are correlated. Results show that the variability of the intensity is correlated with the
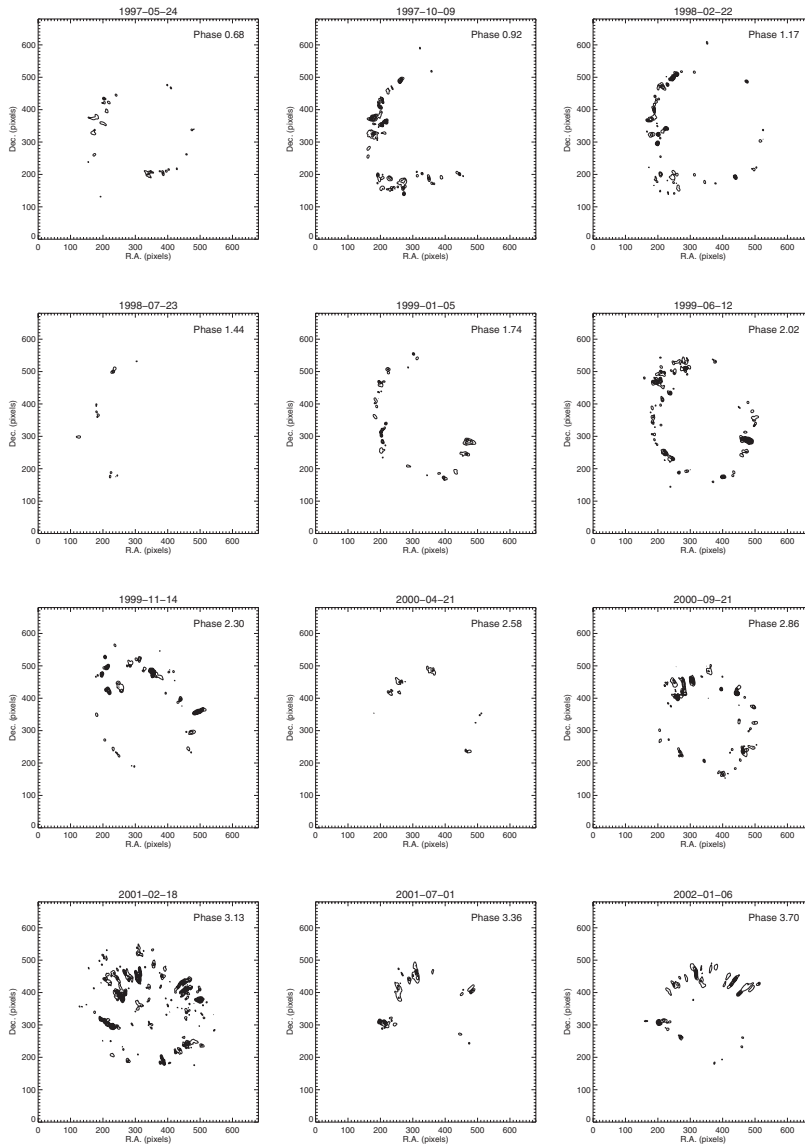
Figure 2: A collage of the total intensity frames. The phase of the frame is written at the top write of each contour plot and the date that the data were taken at the top of each frame. The maps correspond to frames 1,11,21,31,41, 51,61,71,81,91,101 and 111 from the movie. Lower contour value is 1 Jy and the step between each contour is 2.22 Jy until a maximum value of 45.5484 Jy.

pulsation of the star, exhibiting a similar lag to the width. On the other hand the maser and optical fluxes are not correlated. Although the maser intensity follows the pulsation of the star, it does not follow the changes in the optical light; a more intense cycle in the radio is not accompanied by stronger optical fluxes. As a matter of fact, all cycles appear quite uniform with regard to their flux variations in the optical while the maser emission becomes stronger from cycle to cycle.

3.3. *Velocities*

Each cycle is quite different kinematically, and velocity maps reveal the complicated kinematics of the extended atmosphere in the region where the masers are located. During the first and second cycles the maser features appear to move along the line of sight with velocities close to the systemic. This behaviour changes dramatically during the last two cycles where blue- and red-shifted masers seem to dominate the perimeter of the ring and systemic components are absent; there is no gradient, so rotation is not evident. Velocities tend to be blended and in the same portion of the ring both blue and red-shifted masers can be dominant. A characteristic property of the filaments is a velocity gradient along their axes always toward the systemic velocity.

3.4. *Shock Waves*

It is generally believed that shock waves are created in each cycle, when the star is at its maximum. In order to examine the existence of shock waves in the extended atmosphere of TX Cam and their contribution to the overall structure of the ring, we examined the relative position of a shock wave to some key features. As mentioned before there are features that deviate from the ordered flow and they appear at several occasions in the movie as bouncing components or splits in the ring structure. We used for the shock velocity the value graphically calculated by Gonidakis *et al.* (2010), a distance of 390 pc (Olivier, Whitelock & Marang 2001) and a value for the radius of TX Cam of $R_\star = 7.3 \times 10^{13}$ cm at $\phi = 0.939$ (Pegourie 1987). Our results show that the kinematics of all these features can be attributed to their encounter with a shock wave.

References

Diamond, P. J., Kembal, A. J., Junor, W., Zensus, A., Benson, J., & Dhawan, V. 1994, *ApJ*, 430, 61

Diamond, P. J. & Kembal, A. J. 2003, *ApJ*, 599, 1372

Gonidakis, I., Diamond, P. J., & Kembal, A. J. 2010, *MNRAS*, 406, 395

Kemball, A. J. & Diamond, P. J. 1997, *ApJ*, 481, L111

Kemball, A. J., Diamond, P. J., & Cotton, W. D. 1995, *A&AS*, 110, 383K

Olivier, E. A., Whitelock, P., & Marang F. 2001, *MNRAS*, 326, 490

Pegourie, B. 1987, *Ap&SS*, 136, 133